

DOI: 10.5281/zenodo.1409798

THE DIFFERENT INFLUENCE OF NANO MATERIALS ON PIGMENTS

Kholod K. Salama¹, Mona F. Ali², Said M. El-Sheikh³

¹*National Museum of Egyptian Civilization, Cairo, Egypt*

²*University of Cairo, Department of Archaeological Conservation, Faculty of Archaeology, Cairo, Egypt*

³*Nano-Structured Materials and Nanotechnology Division, Advanced Nano-Materials Department
Central Metallurgical Research & Development (CMRDI), P.O.Box 87 Helwan, 1, Elfelezat Street, El-
Tebbin, Helwan 11421 Cairo, Egypt*

Received: 17/05/2018

Accepted: 20/06/2018

Corresponding author: Kholod K.Salama (kholodkhairy@yahoo.com)

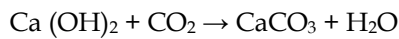
ABSTRACT

Using nano-materials suspension in iso-propanol in conservation field is proved its success. In this paper three nano-materials suspension in ethanol were used to observe its influence on black and red pigments of an Egyptian Coptic fresco model from Saint Jeremiah Monastery obtained from sixth or seventh century AD. Scanning electron microscope (SEM), X-Ray diffraction, Fourier transform infrared and spectrophotometer were used to determine the visual properties of the treated model. The results showed that the addition of nano-materials an obvious change in colours was detected and the mechanical properties of the treated models was improved.

KEYWORDS: Nano-materials, Characterization, Pigment, Application, St Jeremiah Monastery

1. INTRODUCTION

All polymers such as Paraloid B 72 – unfortunately still used in all conservation laboratories until now. They turn to yellow after 20 years at least. In the last decades (Dietemann *et al.*, 2009), in order to avoid these disadvantages, a new way for consolidation appeared using of nano-lime dispersions (usually 2-propanol) has been developed by the Florence Team at the CSGI (Center for Colloid and Surface Science) (Baglioni *et al.*, 2012). This new method has been mainly used to support the mechanical properties. It exhibits a good mechanical properties due to the nano-lime accompanied with the carbon dioxide in the surrounded air to produce new calcium carbonate which filled the gaps and connected the compounds to each other (Bajer, 2007), as the following reaction:



This technique considered very useful in cases of surface color powdering for mural paintings, consolidation and pre-consolidation treatments Once the Ca(OH)_2 nanoparticles penetrate easily into the porous matrix, of the objects (lime stone or in mortars) without any cares of the water content (Blee *et al.*, 2008). The high retention of this absorbed water favors the correct carbonation with formation of a new CaCO_3 crystal network that embeds the detached quartz grains (Baglioni *et al.*, 2006) In the present work the Ca(OH)_2 , CaCO_3 and SiO_2 nano-materials homogeneously dispersed were studied. Scanning electron microscopy (SEM) were used to characterize the influences of nano-materials on pigments. Application to the Coptic Monastery of St Jeremiah in Saqqara is made (Salama *et al* 2017).

2. MATERIALS

All the chemicals were of analytical grade and were used without further purification. The materials required nano calcium hydroxide, nano calcium carbonate and nano silicon dioxide they were purchased from nano tech company Ltd.

The nano calcium hydroxide synthesis was according to Daniel *et al.*, (2012), the nano calcium carbonate synthesis according to Morsy *et al.*, (2014) and nano calcium carbonate synthesis according to Ibrahim *et al.*, (2010). Water was purified by a Millipore Elix 3 apparatus: the resistance of the ultra-pure water was 18 M Ω .cm.

Preparation of the mixed nano-materials system was carried out with two (2) gm of nano-material in ethanol (initial concentration 20 g/L). The composition and the appearance of the obtained mixed system are listed in Table 1.

Table 1: The composition and the appearance of the obtained mixed system

The mixed nano-material system			
Nanomaterial	SiO_2	CaCO_3	Ca(OH)_2
Weight	2	2	2
Ethanol	98	98	98

3. METHODS AND CHARACTERIZATION

3.1. The painting layer condition

The current fresco painting numbered 8425 is stored in the Coptic museum and dates back to 5th century AD (Fig. 1) The models were prepared according to the original mural painting as follows: A first layer of tuff layer from a mixture of hydrated lime - calcium hydroxide and coarse sand, a second layer contains fine sand crystal and lime, and the final layer is the pigments. The pictorial layer suffered from severe loss and color change around the lost areas (Casadio, 2000) and the whole fresco painting suffered from weakness from vital cracks. The three models of Egyptian Coptic fresco were exposed to artificial aging to create similar conditions for the original fresco painting then they were treated with three different system described in Table 1. The models of Coptic fresco paintings were treated with the previous components using brushes through Japanese paper (Natali *et al.*, 2014) The models were subjected to different accelerated ageing test to simulate the most common outdoor heritage deterioration processes due to weathering agents (Batterham, 2008).



Figure 1. The original Coptic fresco painting

3.2 SEM Characterization

The morphology was examined by SEM (scanning electron microscope) model Quanta 250 FEG Field Emission Gun) attached with EDX Unit (Energy Dispersive X-ray Analyses) with accelerating voltage 30 K.V., magnification 14x up to 1000000 and resolution for Gun, 1n FEI Company, Netherlands. Sample preparation consisted of application of a superficial

gold film by sputtering to prevent electro-static effects.

3.3 Fourier transform infrared-Attenuated Total Reflectance (FTIR-ATR)

Samples were analyzed with a FTIR spectrometer (Model 6100 Jasco, Japan). Spectra were obtained in the transmission mode with TGS detector and using ATR crystal which represents (2mm/sec) co added scans at spectral region ranging from 4000 to 400 cm^{-1} with 4 cm^{-1} resolution charge.

3.4 X-ray diffraction (XRD)

The X-ray diffraction patterns of the Coptic fresco painting were obtained using a diffract meter (Philips PW 1840), operated at 40 kV and 25 mA, using Cu Ka radiation and a receiving slit of 0.2 mm. The measurements were made at room temperature. Preparation of each sample consisted of grinding it in the dry form, by using a mortar and pestle to obtain a fine powder.

3.5 Colorimetric measurements

Color changes induced by protective products and samples degradation were evaluated by spectrophotometer Optimatch 3100® from the SDL Company. The dimension of the measured area of each sample equals to (1X1) cm^2 . The colour is given in CIE Lab coordinates, L^* corresponding to the brightness (100 = white, 0 = black), a^* to the red-green coordinate (positive sign = red, negative sign = green), and b^* to the yellow-blue coordinate (positive sign = yellow, negative sign = blue). The total color difference ΔE^* between two color stimuli $\Delta E^* = \{(\Delta L^*)^2 + (\Delta a^*)^2 + (\Delta b^*)^2\}$ (Darwish, 2014).

4. RESULTS AND DISCUSSION

The colours which were used in the painting are among the most common and available pigments in the surrounded environment (Buxbaum, 2005). The red color is Hematite, the yellow color is Goethite, the green color is the Malachite, and the black color is the Perollosite.

Those nano materials were mixed with ethanol after testing the color changing after the treatment with isopropanol and ethanol. The isopropanol proved successful as it did not cause any color changing, on the other hand the ethanol caused a little lightness for colours that can be ignored and the evaporation speed of the both are similar but the isopropanol took longer time than ethanol, almost 0.001/second, but for isopropanol it took 0.001-0.002/second. The application of the three nano-materials caused changes in the visual properties, such as changes in due to the treated models which can be tested by using spectrophotometer. On other hand, the nano-materials improved the mechanical properties of the treated models, as the nano-materials increase the models strength to the exogenous factors as the mechanical properties were tested using the hardness tester and the bursting strength detector .

4.1. The visual properties and the changes of colour after treatment

The purpose of comparison the changes of visual colours before (2A) and after treatment (2B-C) to detect the change of brightness caused by treatment. The pigments after treatment with nano-materials appeared with an opaque layers on them as shown in Figure 2(B-C). the change in red and black color in case of application with nano calcium hydroxide in figure (2B) can be ignored. On other hand in cases of nano calcium carbonate and nano silica Fig. 2 (C,D).

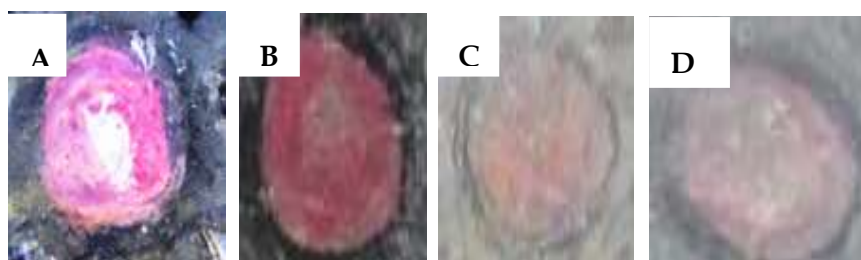


Figure 2: A) Untreated model and the red and black colours after treatment with B) nano-calcium hydroxide C) nano-silica D) nano-calcium carbonate.

4.2. SEM

Fig.3 (A-H) revealed the red pigment before treatment with nano-materials. The red pigments particles appeared non-homogenous but after treatment with nano-calcium hydroxide the inte-

rior structure combined together. Yet in the case of nano-calcium carbonate and nano-silica it appeared as filler inside the structure of red pigment.

The same above changes appeared with the black pigment.

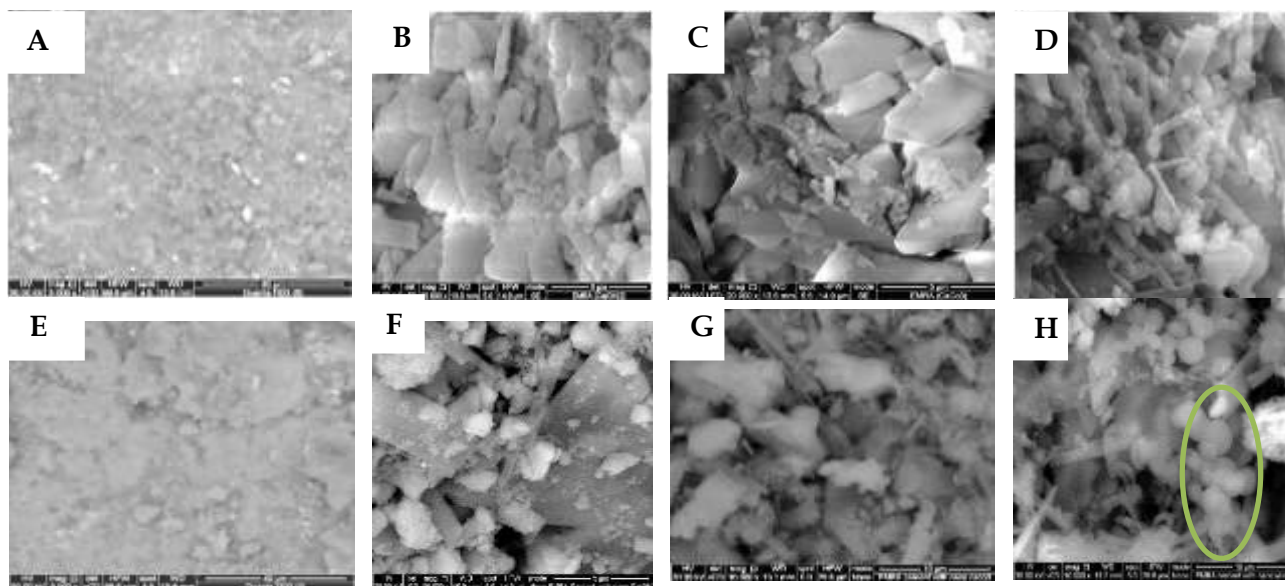


Figure 3: SEM images of pigment red A) untreated pigment red appeared with less cohesion B) $\text{Ca}(\text{OH})_2$ during the carbonation process and combining the interior structure, C) nano-silica filling the gaps, D) nano-calcium carbonate filling the gaps and SEM images of pigment Black, E) untreated pigment black appeared with less cohesion, F) $\text{Ca}(\text{OH})_2$ during the carbonation process and combining the interior structure, G) nano-silica appeared filling gaps, H) nano-calcium carbonate appeared filling gaps (circle revealed the presence of nanomaterial in the interior structure.)

4.3 FTIR

Fig. 4A-H shows FTIR spectra of: A) untreated pigment red, B) $\text{Ca}(\text{OH})_2$, C) nano-silica, D) nano-calcium carbonate, E) untreated pigment black, F) $\text{Ca}(\text{OH})_2$, G) nano-silica, H) nano-calcium carbonate. The FTIR of untreated pigment (Fig. 4A) revealed that at least one strong absorption band from C-O stretching at 1415 cm^{-1} calcite, the band is smooth, symmetrical, and broad. Carbonate bending vibrations produce sharp bands in the region of $900\text{-}650\text{ cm}^{-1}$. These bands show measurable frequency deviations corresponding to the attached cation. For example, the out-of-plane bending vibration for calcium carbonate (calcite) occurs at 873 cm^{-1} , SO_4 bending and stretching band at $667, 1107\text{ cm}^{-1}$, anti-symmetric and symmetric O-H stretching bands of gypsum at $3522, 3399\text{ cm}^{-1}$. And the major distinguished Fe-O for Hematite for red pigment appeared on 449 cm^{-1} Fig. 4 (B-C) after application with three nano-materials there are no any changes happened in the color as it is still appeared in 450 cm^{-1} . According to Fig. 4-E black pigment appeared with calcium carbonate and gypsum and the black color appeared as Mn-O for Perollosite at 720 cm^{-1} . Fig. 4 (F-H) shows that, after the application of three nano-materials, no change took place in the color due to the stretching area of Mn-O 720 cm^{-1} .

4.4 XRD

Fig. 5 A-H shows the x-ray Diffraction (XRD) of the treated pigments (red and black) with the three nano-materials. The XRD data revealed that the calcite and gypsum are more major components with Hematite in D value 2.5190 in case of red pigment and Perollosite in D value 2.440 in case of black pigment treated with three nano-material. From Fig. 5A-H it was noticed that the intensities of calcium carbonate XRD peaks which converted from calcium hydroxide are higher than the intensities of the nano-calcium carbonate (Fig. 5B) which means the size are increased of as seen in SEM image Fig. 3B. On the other hand, it was observed that the samples treated with nano-silica (Fig. 5D) revealed that the intensities of original calcium carbonate of the model sample are less than other nano-carbonate sample. After all, the comparison between prior and later stage of the two pigments the red and black color appears on the same area like the nano-materials never affect the nature of pigments.

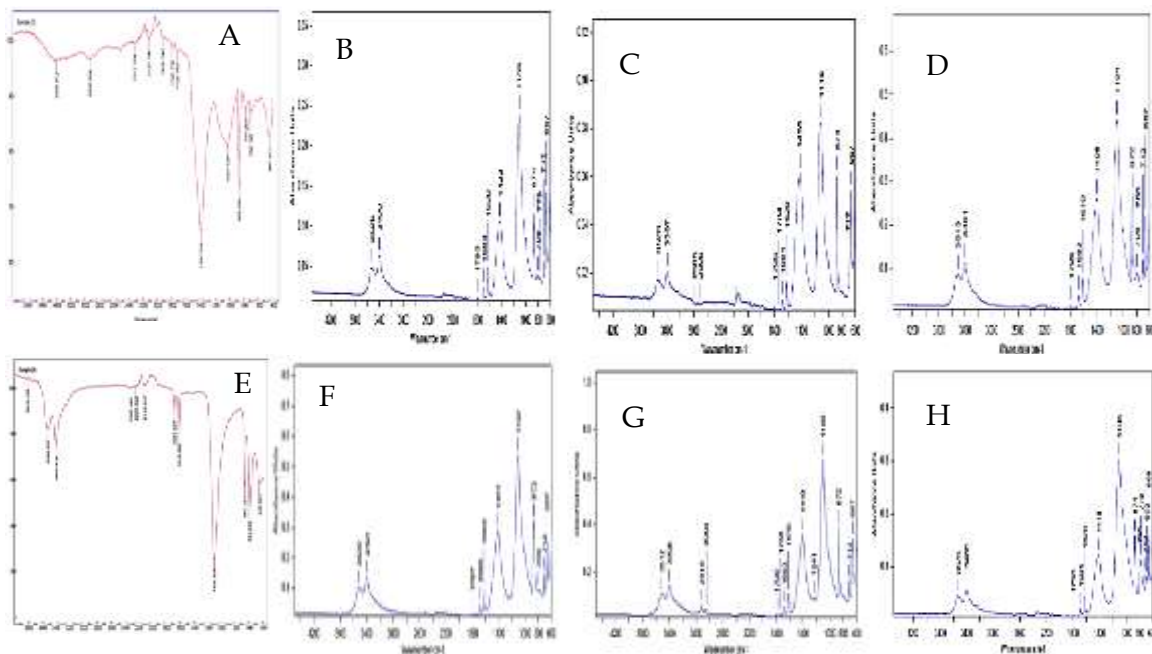


Figure 4A-H: FTIR spectra of A) untreated pigment red B) $\text{Ca}(\text{OH})_2$, C) nano-silica, D) nano -calcium carbonate, and (E) untreated pigment black F) $\text{Ca}(\text{OH})_2$, G) nano-silica, H) nano-calcium carbonate.

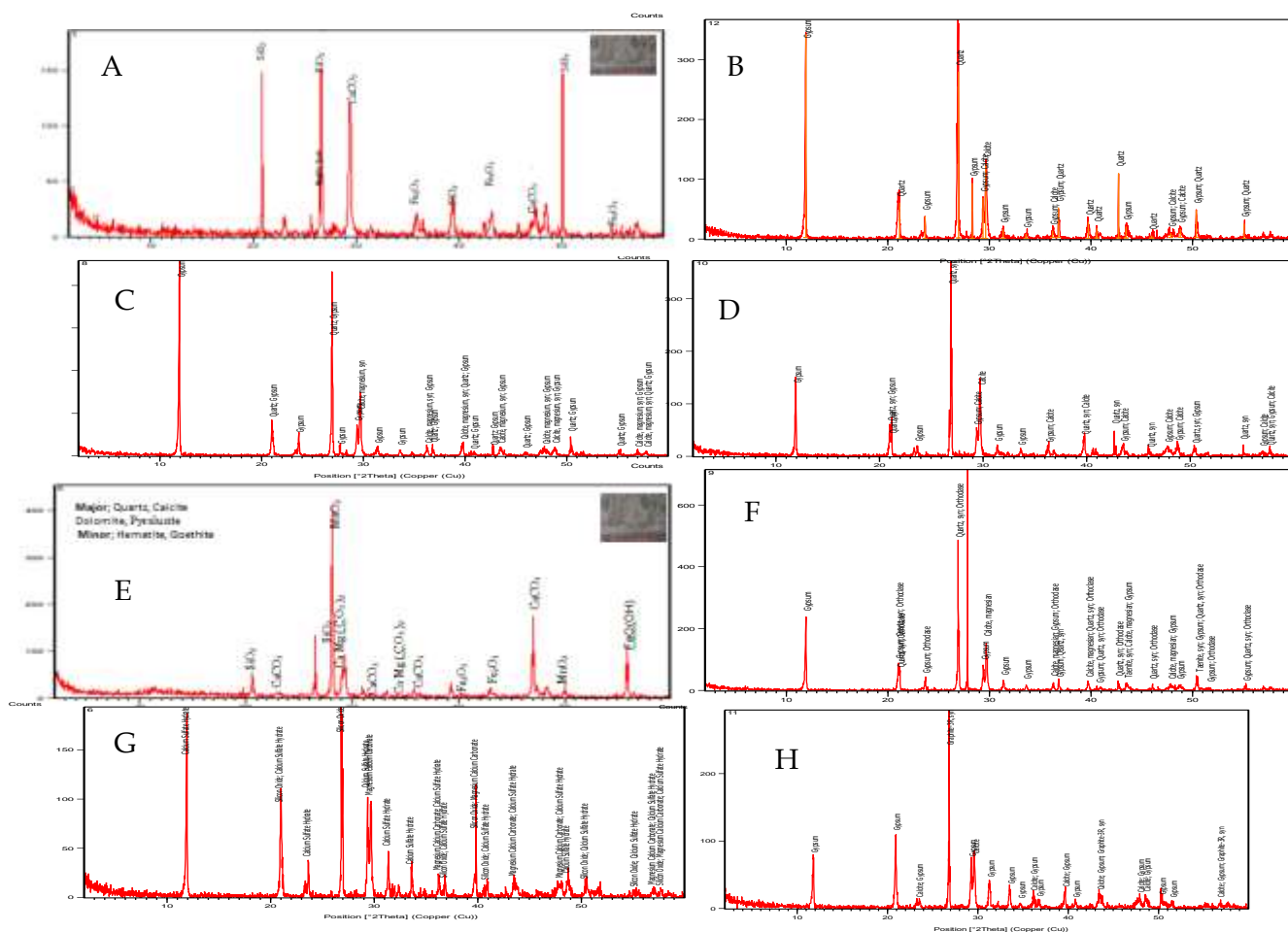


Figure 5: X-ray Diffraction (XRD) of the red and black pigments before and after treatment with three nano materials A) untreated pigment red with Hematite appeared on 2.5190 D value B) $\text{Ca}(\text{OH})_2$, C) nano-silica, D) nano -calcium carbonate, and (E) untreated pigment black Perlolosite appeared on D value 2.440 F) $\text{Ca}(\text{OH})_2$, G) nano-silica, H) nano-calcium carbonate.

4.5 Spectrophotometer

Table 2 shows the color variation promoted on the models after treatment with nano-lime, nano-silica and nano-calcium carbonate ΔL^* is the variation in luminosity, Δa^* is the variation in the red-green parameter, Δb^* is the variation in the blue-yellow parameter and ΔE^* is the total color difference. It displays the color variations of the treated models for the tested treatments, the most important contribution came from $L^* a^* b^*$ where L^* represents light-

ness (0% black, 100% white), a^* redness-greenness, and b^* yellow-blueness. For this work the values of $a^* > 0$ and $b^* > 0$ which represent the colours red and yellow, respectively. The yellow color of untreated models falls within the range: $L^* -9.88$, $a^* 3.24$ and $b^* 0.062$. In general, treatments of nano-material led to a darkening of the models surfaces. For nano-calcium hydroxide for example, the L^* dropped by -10.37.

Table 2: Coordinates of color obtained by using spectrophotometer

Color	ΔL^*	Δa^*	Δb^*	ΔE^*	Observations
Black untreated	-0.76	-0.08	2.22	2.35	$10 > \Delta E > 5$
Red untreated	1.60	0.87	1.09	2.12	In the untreated samples.
Black Ca(OH) ₂	10.55	0.05	0.39	10.56	ΔE values indicated that this variation is the same of the treatments
Red Ca(OH) ₂	8.09	0.56	10.46	13.24	
Black SiO ₂	-16.88	1.15	-4.47	17.50	
Red SiO ₂	-38.78	-0.17	-8.08	39.61	
Black CaCO ₃	-1.58	0.21	-10.09	3.99	
Red CaCO ₃	-3.26	1.67	6.47	7.43	

The color of models treated with nano-materials were observed to alter slightly after the treatment, ΔE scale in stone materials conservation for consolidation or for preventing microbial growth (Fatma M. Helmi, et al, 2007) is as follow:

- $\Delta E < 0.2$: not perceptible difference
- $0.2 < \Delta E < 0.5$: very small difference
- $0.5 < \Delta E < 2$: small difference
- $2 < \Delta E < 3$: fairly perceptible difference
- $3 < \Delta E < 6$: perceptible difference
- $6 < \Delta E < 12$: strong difference
- $\Delta E > 12$: different colors

In this respect red and black colours in the treated models with nano-materials before and after aging have no acceptable ΔE values where it ranges between 2.12 and 10.42. Other coloured samples treated with nano-materials were not fitting in these limits i.e., have ΔE values between 44.63 and 5.42 depending on their chemical composition. The completed data are listed in Table 2, a clear change in

surface color was observed visually. The average b^* and a^* values increased and the models appears red-orange colored after the treatment. This discoloration very probably results from the accumulation of nano-materials on the surfaces (X-rite, 2007)

5. CONCLUSION

This study focused on the interactions between nano calcium hydroxide, nano-silica and nano calcium carbonate applied on the St Jeremiah Coptic Monastery in Saqqara wall paintings. The nano-calcium hydroxide turned into calcium carbonate as the known carbonation process and Both nano silicon Nano silica and nano-calcium carbonate used as filler as they filled the gaps inside the structures of the red and black pigment as SEM images showed. The application of those Nano-materials on the consolidation of pigments caused a visual difference in colours compared with untreated ones as detected by the spectrophotometer.

REFERENCES

- Batterham I., Rai R. (2008) A comparison of artificial aging with 27 years of natural aging 2008 AICCM Book, Paper and Photographic Materials Symposium, 2008, pp.1-9.
- Baglioni P., Giorgia R., Chelazzia D. (2012) Nano materials or the conservation and preservation of movable and immovable art works, *Progress in cultural heritage Preservation*, EUROMED, pp313-318.
- Brajer I. (2007) Problems with past conservation treatments on the wall church paintings in and lose in a research and development report from the workshop November 2-3, Österbybruk, Upland, Sweden, pp.1-72.
- Blee A., Martin J.G. (2008) Nanoparticles and the conservation of cultural heritage, *Materials Forum*, 32, pp.121-128.
- Baglioni P., Giorgi R. (2006) Soft and hard nano-materials for restoration and conservation of cultural heritage, *Soft Matter*, 2006, pp. 293-303.
- Casadio F., Colombo C., Toniolo L. (2000) Detaching Methodology for fresco Painting, In: 9th International Congress on

- Deterioration and conservation of stone, Venice June 19- 24, *Journal of Cultural Heritage*, pp. 739-747.
- Darwish S.S. (2013) Evaluation of the effectiveness of some consolidates used for the treatment of the Sixth century Egyptian cemetery wall painting, *International Journal of Conservation Science*, 4(4), pp.413-422.
- Daniele V., Taglieri G. (2012) Synthesis of Ca(OH)₂ nanoparticles with the addition of Triton X-100. Protective treatments on natural stones: Preliminary results, *Journal of Cultural Heritage*, 2012, pp.40-46.
- Dietemann P., Higgitt C., Kalin M., Edelmann M.J., Knochenmuss R., Zenobi R. (2009) Aging and yellowing of triterpenoid resin varnishes e Influence of aging conditions and resin composition, *Journal of Cultural Heritage*, pp.30-40
- Helmi, F.M, Naglaa M. Ali, Sahar M. Ismael (2015) Nanomaterials for The Inhibition of Microbial Growth on Ancient Egyptian Funeral Masks. *Mediterranean Archaeology and Archaeometry*, Vol. 15, No 3, pp. 87-95.
- Ibrahim I.A.M, Zikry A.A.F., Sharaf M.A., (2010) Preparation of spherical silica nanoparticles: Stober silica, *Journal of American Science*, 6(11), pp.986-989.
- Morsy F.A., El-Sheikh S. M., Barhoum A., (2014) Nano-silica and SiO₂/CaCO₃ nano composite prepared from semi-burned rice straw ash as modified papermaking fillers, *Arabian Journal of Chemistry*, pp.1-11 (DOI: 10.1016/j.arabjc.2014.11.032)
- Natali I., Saladino M.L., Andriulo F., Martino C., Caponetti E., Carretti E., Dei L.(2014) Consolidation and protection by nanolime: recent advances for the conservation of the graffiti, Carceri dello Steri Palermo and of the 18th century lunettes, SS. Giuda e Simone Cloister, Carniola (Emboli), *Journal of Cultural Heritage*, pp.151-158.
- Salama, K,K, Mona F. Ali, S.M. El-Shiekhn (2017) Reconstruction of Monastery Saint Jeremiah computer-aided design model. *SCIENTIFIC CULTURE*, Vol. 3, No. 1, pp. 11-14 (DOI: 10.5281/zenodo.192839)
- X-rite.com (2007) A guide to understand color communication, x-rite incorporate, p.1-26